

Systematically convergent basis sets for transition metals.

I. All-electron correlation consistent basis sets for the 3d elements Sc–Zn

Nikolai B. Balabanov^{a)} and Kirk A. Peterson^{b)}

Department of Chemistry, Washington State University, Pullman, Washington 99164-4630

(Received 25 February 2005; accepted 14 June 2005; published online 18 August 2005)

Sequences of basis sets that systematically converge towards the complete basis set (CBS) limit have been developed for the first-row transition metal elements Sc–Zn. Two families of basis sets, nonrelativistic and Douglas-Kroll-Hess (-DK) relativistic, are presented that range in quality from triple- ζ to quintuple- ζ . Separate sets are developed for the description of valence ($3d4s$) electron correlation (cc-pVnZ and cc-pVnZ-DK; $n=T, Q, 5$) and valence plus outer-core ($3s3p3d4s$) correlation (cc-pwCVnZ and cc-pwCVnZ-DK; $n=T, Q, 5$), as well as these sets augmented by additional diffuse functions for the description of negative ions and weak interactions (aug-cc-pVnZ and aug-cc-pVnZ-DK). Extensive benchmark calculations at the coupled cluster level of theory are presented for atomic excitation energies, ionization potentials, and electron affinities, as well as molecular calculations on selected hydrides (TiH, MnH, CuH) and other diatomics (TiF, Cu₂). In addition to observing systematic convergence towards the CBS limits, both $3s3p$ electron correlation and scalar relativity are calculated to strongly impact many of the atomic and molecular properties investigated for these first-row transition metal species. © 2005 American Institute of Physics. [DOI: 10.1063/1.1998907]

I. INTRODUCTION

Chemistry involving transition metal elements is extremely rich and ranges from materials science and catalysis to biology and problems of environmental concern. Obtaining accurate descriptions of these systems, however, can be very challenging for *ab initio* electronic structure theory. On the one hand, the electron correlation problem in transition-metal-containing systems can be extremely demanding due to open d shells and a concomitant high density of electronic states. Advances in coupled cluster and multireference methods, as well as density functional theory, have come a long way towards addressing this problem. On the other hand, the resulting accuracy of any correlated electronic structure calculation can be highly dependent on the one-particle basis set used to represent the molecular orbitals. In particular, the coupling between the correlation method and the basis set can lead to erratic results that limit our understanding of the intrinsic errors associated with the chosen computational method. Certainly it is also the case that the systematics of basis set incompleteness must be understood at a fundamental level in order to obtain the kind of accurate results now possible for processes involving only main group elements in the general areas of chemically accurate thermochemistry and *ab initio* spectroscopy and dynamics.

One of the major advances in the *ab initio* calculation of molecular electronic structure over the last 15 years has been the development of Gaussian basis sets that exhibit systematic convergence towards the complete basis set (CBS) limit. Following the work of Jankowski *et al.*¹ and the introduction of atomic natural orbital (ANO) basis sets by Almlöf and

Taylor,² Dunning reported³ the family of correlation consistent (cc) basis sets for the first-row elements, denoted cc-pVnZ with $n=D, T, Q, 5$, which allowed for the systematic extension of the one-particle basis set towards the CBS limit in correlated calculations. These sets have revolutionized quantum chemistry in areas such as *ab initio* thermochemistry and spectroscopy since they can yield accurate CBS limit results, i.e., the exact solution of, e.g., the coupled cluster equations. In particular, the errors associated with the method and basis set can be decoupled, which greatly facilitates error estimates. Since the original work of Dunning, the family of correlation consistent basis sets has been extended to include all of the p -block elements of groups 13–18,^{4–6} as well as extensions to describe anions, van der Waals interactions, and core-valence electron correlation.^{7,8}

While correlation consistent basis sets have become the de facto standard for accurate *ab initio* calculations on systems involving main group elements, a similar choice does not generally exist for the transition metals. Numerous basis sets are available for the first-row transition metal elements, both large and small,^{9–14} yet except for a few selected elements^{12,14,15} none form a family of basis sets capable of systematically converging to the CBS limit like the correlation-consistent sets. In the present work, basis sets exhibiting systematic convergence towards both the Hartree-Fock (HF) and correlated CBS limits are developed for the 3d transition metal elements, Sc–Zn. Series of basis sets ranging in quality from triple- ζ to quintuple- ζ have been determined using both nonrelativistic (NR) and relativistic Douglas-Kroll-Hess¹⁶ (DKH or DK) calculations; separate sets for valence-only correlation, $3d4s$, as well as those including the effects of outer-core correlation, $3s3p3d4s$, are included. Analogous double- ζ basis sets have not been in-

^{a)}Electronic mail: nick@mail.wsu.edu

^{b)}Electronic mail: kipeters@wsu.edu

cluded in the present work due to the ready availability of basis sets of this size. The resulting basis sets of this work, which also include those extended by additional diffuse functions for the treatment of anions and weak interactions, have been used in benchmark calculations at the coupled cluster level of theory for various atomic and molecular spectroscopic and thermochemical properties. The details of the basis set optimizations is described in Sec. II, while the results of the atomic and molecular benchmark calculations are presented in Sec. III. The conclusions drawn from the present work are summarized in Sec. IV.

II. BASIS SET CONSTRUCTION

The methods used for the exponent optimizations closely followed those recently used in the construction of cc-pVnZ-PP basis sets for the post- d elements.⁶ Namely, a conjugate gradient algorithm¹⁷ using double-sided numerical derivatives was employed with energy gradients converged to better than 1×10^{-6} a.u. The MOLPRO program suite¹⁸ was used throughout and only the pure spherical harmonic components of the dfg angular momentum functions were utilized. All HF and configuration interaction (CI) natural orbitals were full symmetry equivalenced.

Overall, the optimization of correlation consistent basis sets for the transition metals should follow a similar procedure as that used previously with main group elements, i.e., several HF sets that range in accuracy from a double- or triple- ζ description of the valence orbitals to near the HF limit are first optimized and then appropriate shells of correlating functions are determined. However, as discussed previously by several authors (see Refs. 13 and 19–21), the development of accurate basis sets for transition metals should involve addressing a number of issues that do not generally exist for main group elements. In particular, most of the transition metal (TM) elements have several important low-lying electronic states that contribute to bonding in molecules, namely, configurations of the type $ns^2(n-1)d^{m-2}$, $ns(n-1)d^{m-1}$, and $(n-1)d^m$, where m is the number of valence electrons. Optimization of basis function exponents for just one of these configurations, e.g., the atomic ground state, can introduce significant bias into the results, especially since the ns orbital generally has a very different radial extent than the $(n-1)d$ orbital. In addition, the np valence orbitals are unoccupied for the atoms, but can be important for bonding in molecular systems. Lastly, the radial extent of the outer-core $(n-1)sp$ shell is very similar to that of the valence $(n-1)d$ shell, which can lead to strong core-valence correlation effects.

In the case of all-electron basis sets for the first-row transition metals (Sc–Zn), Bauschlicher and Taylor,²⁰ Bauschlicher,¹³ and Pou-Amérgo *et al.*²¹ have carefully addressed the issues noted above for accurate correlated calculations within the framework of ANO basis sets. Each of these studies was based on the large spd Hartree-Fock basis sets optimized by Partridge²² for the $4s^23d^{m-2}$ states of the atoms. Several diffuse p functions were then added in an even-tempered²³ fashion to describe the $4p$ orbital, as well as an additional diffuse d -type function. The latter was to ac-

count for a possible bias in the original HF d set against the $4s3d^{m-1}$ configuration.¹⁹ ANO-contracted correlating functions of dfg symmetry were then added to these sets, and these were optimized for the average energy of up to three electronic states of the atoms. In the work of Pou-Amérgo *et al.*,²¹ ionic states and calculations with small external electric fields applied to the neutral atoms were also used in the averaging procedure. More recently, these ideas have been extended to correlation consistent polarization functions by Bauschlicher¹⁴ and Ricca and Bauschlicher¹² in basis sets for Ti and Fe, respectively. A very different optimization scheme has recently been reported by Noro *et al.*,¹¹ where the exponents and contraction coefficients were optimized to closely reproduce large basis set ANOs from state-averaged CI calculations of the $4s^23d^{m-2}$ and $4s3d^{m-1}$ states.

The present work incorporates some of the strategies used in these previous studies, particularly in regards to the optimization of exponents for the average energy of several atomic states. In regards to the primitive HF spd sets, s sets that were optimized for just the $4s^23d^{m-2}$ atomic states were chosen, since this procedure has been shown to stabilize triple- ζ distributions describing the valence $4s$ orbital.²⁴ It might be noted that this choice of electronic state for the s exponent optimizations, $4s^23d^{m-2}$, is not the same as the ground states of the Cr and Cu atoms, $4s^13d^{m-1}$. Initially the p sets were also optimized for just the $4s^23d^{m-2}$ states, but then the most diffuse exponent was replaced by three exponents optimized for the lowest term corresponding to a $4s^23d^{m-3}4p^1$ occupation. Previous works that had explicitly optimized additional HF $4p$ functions had done so for either the $3d^{m-2}4p^2$ (Ref. 9) or $4s3d^{m-2}4p^1$ states,²⁵ but it has been noted previously²² that these procedures can yield exponents that are too diffuse for molecular calculations. In our preliminary work, this did not seem to be the case when the excited state that was used for the optimizations kept the $4s$ orbital doubly occupied. In particular, this scheme also appeared to lead to very consistent p exponent distributions across the row. Lastly, for the optimization of d -type HF sets, these exponents have been optimized for the average HF energy of three states: the $4s^23d^{m-2}$, $4s^13d^{m-1}$, and $3d^m$ [of course, only two states for Cu ($m=11$) and one state for Zn ($m=12$)]. This procedure naturally led to a diffuse d function that described states with higher d occupations without resorting to either just an even-tempered extrapolation of a $4s^23d^{m-2}$ optimized basis set as was done in most previous works or optimizations on one particular d -excited state, e.g., the $3d^m$ state as in Ref. 19.

Specifically, the sp primitive sets used for the current TZ and QZ basis sets were taken from the work of Partridge,^{22,26} ($20s14p$) and ($22s16p$), respectively, with the subsequent modification of the outermost p exponent as described above. These were paired with ($8d$) and ($11d$) sets fully optimized in the present work as described above. In the case of the 5Z basis sets, sufficiently large sp sets were not available in the literature, so optimizations were carried out for a ($28s18p12d$) set. However, because of the inherent inaccuracies of the numerical gradients used in this work, particularly in regards to the very large exponent, tight s functions occurring in these basis sets, reliable *full* optimizations of the

TABLE I. Neutral atom states (cation and anion ground states in square brackets) used in the basis set optimizations and calculations of the present work with their corresponding electronic configurations. Note that m refers to the total number of valence electrons ($4s$ and $3d$).

	m (neutral)	$[\text{Ar}]4s^23d^{m-2}$	$[\text{Ar}]4s^13d^{m-1}$	$[\text{Ar}]4s^03d^m$	$[\text{Ar}]4s^23d^{m-3}4p^1$
Sc	3	$^2D^a$	$^4F, [^3D]^b$	4F	$^2P, [^1D]^c$
Ti	4	$^3F, ^a [^4F]^c$	$^5F, [^4F]^b$	5D	3D
V	5	$^4F, ^a [^5D]^c$	6D	$^6S, [^5D]^b$	4G
Cr	6	$^5D, [^6S]^c$	$^7S^a$	$^5D, [^6S]^b$	5G
Mn	7	$^6S^a$	$^6D, [^7S]^b$	4F	6F
Fe	8	$^5D, ^a [^4F]^c$	$^5F, [^6D]^b$	3F	7P
Co	9	$^4F, ^a [^3F]^c$	4F	$^2D, [^3F]^b$	6D
Ni	10	$^3F, ^{a,d} [^2D]^c$	3D	$^1S, [^2D]^b$	5F
Cu	11	$^2D, [^1S]^c$	$^2S^a$	$[^1S]^b$	4D
Zn	12	$^1S^a$	$[^2S]^b$...	3P

^aNeutral atom ground state (in the absence of spin-orbit coupling).

^bCation ground state (in the absence of spin-orbit coupling).

^cAnion ground state (in the absence of spin-orbit coupling).

^dThe lowest-energy j -averaged state in Ni corresponds to the $[\text{Ar}]4s^13d^9(^3D)$ state, but the spin-orbit ground state arises from the $[\text{Ar}]4s^23d^8(^3F)$ state.

sp sets were not possible. Test optimizations based on the $22s$ set of Partridge, however, indicated that nearly identical results could be obtained by using a six-term Legendre expansion as described by Petersson *et al.*²⁷ for the inner exponents while the five most diffuse exponents were fully optimized. This procedure was followed to generate $(28s18p)$ primitive sets optimized for the $4s^23d^{m-2}$ atomic states. The most diffuse p exponent was then replaced by three exponents optimized for the lowest $4s^23d^{m-3}4p^1$ states as in the TZ and QZ cases, and all the exponents of the 12d set were fully optimized for the HF average energy of up to three atomic states. For all of the DK relativistic basis sets, TZ–5Z, only the three most diffuse p exponents and the d sets were optimized with the inclusion of the DKH Hamiltonian. Because relativistic effects are less important for these more diffuse functions, the resulting exponents differed only slightly from the NR sets. The final composition of the spd HF primitive sets for the $3d$ transition metal elements obtained in this work are $(20s16p8d)$ for TZ, $(22s18p11d)$ for QZ, and $(28s20p12d)$ for 5Z. Note that the sizes of the current d sets are consistent with HF sets chosen previously for the standard post- $3d$ cc-pVnZ basis sets,⁵ while the present sp sets are slightly larger. In order to minimize bias towards one particular atomic state, these spd sets were generally contracted to $[4s3p1d]$ using atomic orbital (AO) coefficients obtained from state averaging up to three sets of HF density matrices (DK-HF for the relativistic basis sets), $4s^23d^{m-2}$ and $4s^13d^{m-1}$ states for Sc–Co and Cu, these two plus the $3d^{10}$ for Ni, and just $4s^23d^{10}$ for Zn. An additional contracted p function was also included to describe the $4p$ orbital using the AO coefficients from the lowest $4s^23d^{m-3}4p^1$ state. Designations of all the atomic states used in the present work are explicitly shown in Table I. It should also be noted that a finite nuclear model was not used in the present DK calculations, and hence these basis sets may have to be recontracted for use in programs such as GAUSSIAN03 where this model is employed by default.²⁸

A. Valence-only correlation, cc-pVnZ basis sets

With the HF sets determined, the next step in the construction of correlation consistent basis sets for valence electron correlation was to ascertain the proper shells of correlating functions to add to produce cc-pVTZ, cc-pVQZ, and cc-pV5Z basis sets. In the case of $fghi$ angular momentum functions, Ricca and Bauschlicher¹² and Bauschlicher,¹⁴ as well as Pykavy and van Wuelen,¹⁵ utilized the expected, traditional patterns of $2f1g$ for TZ, $3f2g1h$ for QZ, and $4f3g2h1i$ for 5Z in their valence correlation consistent basis sets for Ti, Fe, and V. In the present work this prescription has been analyzed with calculations on the $4s^23d^8$ state (3F_g) of the Ni atom. Beginning with the QZ-DK primitive set contracted to $[8s7p5d]$, even-tempered sequences of f , g , h , and i angular momentum functions were successively added. The incremental valence ($4s3d$) correlation energies were obtained using the singles and doubles configuration interaction (CISD) method with the DKH Hamiltonian. These results are shown in Fig. 1. Within each angular momentum symmetry type, regular, nearly exponential convergence is observed. Correlation consistent shell groupings, however, are not very clear, especially for the first few functions. The first f function is the most important from an energetic standpoint and hence it could be chosen for a DZ basis set. The second f function, however, yields much more correlation energy than the first g function. In contrast, the next two expected groupings, $3f2g1h$ (QZ) and $4f3g2h1i$ (5Z), exhibit more typical correlation consistent behavior. While these results might suggest an alternative definition for the valence TZ correlation set, the traditional correlation consistent shells have been retained in this work since then both the radial and angular spaces are increased with each successive basis set. As shown below in the atomic and molecular benchmark calculations, this choice does appear to lead to well-behaved convergence properties. Actually it has been shown previously,²⁹ and confirmed in the present work, that more regular correlation consistent behavior is observed when $3s3p$ correlation is included with $4s3d$, but this occurs

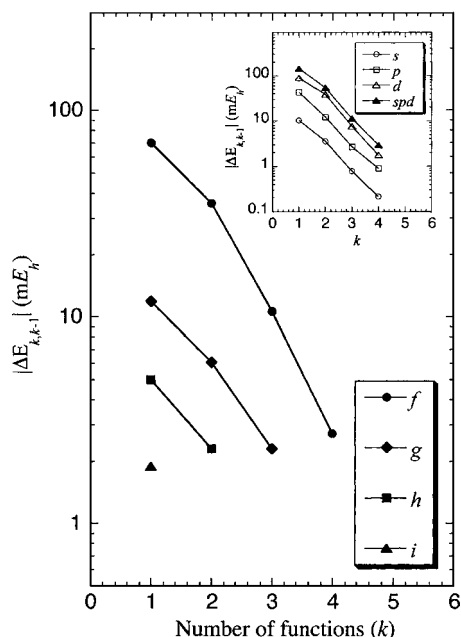


FIG. 1. Contributions of angular momentum functions to the valence DK-CISD correlation energy in the $4s^2 3d^8 (^3F_g)$ state of the Ni atom. The absolute values of the incremental correlation energy lowerings, $|\Delta E_{\text{corr}}|$, are plotted in mE_h against the number of functions (k) in the expansions of $fghi$ functions in a large spd set. The inset depicts the convergence of correlating s , p , and d functions as well as their total correlation energy contribution as obtained by DK-CISD calculations.

at the expense of the convergence rate for describing valence electron correlation, which is still the most important for molecular calculations. Hence, the present work provides separate basis sets for valence and core-valence correlation (see below). In the final valence basis sets developed here, the even-tempered sequences of $fghi$ functions, $2f1g$ for TZ, $3f2g1h$ for QZ, and $4f3g2h1i$ for 5Z, were optimized for the average CISD energy of the $4s^2 3d^{m-2}$, $4s^1 3d^{m-1}$, and $3d^m$ states for Sc–Ni, while only the first two states and the first state were used for Cu and Zn, respectively.

In addition to determining correlating functions for higher angular momentum symmetries, those of spd type must also be included. In the work of Ricca and Bauschlicher¹² and Bauschlicher¹⁴ several spd functions from the HF set were uncontracted and this same set of functions was used for their TZ, QZ, and 5Z basis sets. In the standard correlation consistent basis sets for the main group elements, functions were also simply uncontracted from the HF sets. The number of uncontracted functions increased systematically from $1s1p1d$ for the DZ sets up to $4s4p4d$ for the 5Z sets for Kr. In the present work a compact representation was also desired, but instead of uncontracting functions from the underlying HF sets, it was determined that it was much more accurate in regards to evenly treating multiple atomic states to use contractions based on CISD atomic natural orbitals. In the cases of Sc–Co and Cu, these were obtained by averaging the symmetry equivalenced CISD density matrices of the lowest atomic states with $4s^2 3d^{m-2}$ and $4s3d^{m-1}$ occupations (cf., Table I). For the Ni atom, the $3d^{10}$ state was also included, while for Zn only the $4s^2 3d^{10}$ ground state was used. This approach provided an accurate

and compact description of the correlation effects involving s , p , and d functions with the advantage of being able to simultaneously describe several low-lying atomic states. The inset to Fig. 1 demonstrates the incremental correlation energy recovery in DK-CISD calculations on the $4s^2 3d^8$ state of Ni as sets of ANOs are added to a contracted $[4s2p1d] + 4f3g2h1i$ basis set. Overall, the convergence is regular and very similar to that of the f -type correlating functions. Hence, a $(2s2p2d)$ set of ANOs was used for the TZ set, a $(3s3p3d)$ set for the QZ, and a $(4s4p4d)$ set for the 5Z. Additionally, in order to provide more flexibility in the final basis sets, the most diffuse Gaussian primitive in each symmetry was also uncontracted in each set. The final contracted cc-pVnZ and cc-pVnZ-DK basis sets designed for correlating the $4s3d$ electrons consisted of $[7s6p4d2f1g]$ for cc-pVTZ(-DK), $[8s7p5d3f2g1h]$ for cc-pVQZ(-DK), and $[9s8p6d4f3g2h1i]$ for cc-pV5Z(-DK).

B. Valence plus outer-core correlation, cc-pwCVnZ basis sets

It is generally well recognized that especially for the early $3d$ transition metals, correlation of the outer-core $3s$ and $3p$ electrons is very important for accurate work. Just as in the case of main group elements, however, additional functions optimal for correlating outer-core electrons should be added to a basis set designed only for valence electron correlation. In the present work, the weighted core-valence scheme of Peterson and Dunning⁸ has been adopted, whereby the intershell, core-valence correlation energy is strongly weighted over the intrashell, core-core correlation energy in the optimization procedure. In order to determine the number and type of functions to add to each valence set to obtain cc-pwCVTZ, cc-pwCVQZ, and cc-pwCV5Z basis sets, numerous test calculations on the atomic ground states of both Ti and Ni were carried out. For the higher angular momentum functions ($fghi$), these results were in general agreement with the previous conclusions of Bauschlicher for the Ti atom,¹⁴ whereby since the optimum correlating functions for valence and valence+ $3s3p$ overlap considerably, the core-valence functions added to the valence basis sets should consist of just one additional function in each angular symmetry present in a $3s3p$ correlating set. Hence with this prescription the cc-pwCVTZ basis would involve adding just one additional f -type function to the cc-pVTZ, the cc-pwCVQZ would add one f and one g , etc. Inspection of the incremental core-valence correlation energies, however, demonstrated that the first tight function of the next highest angular momentum, e.g., a g -type function in the TZ case or an h -type function in the QZ case, actually contributed slightly more correlation energy than those functions of lower angular momentum. This is perhaps due to the focus in this work on the intershell core-valence correlation energy rather than the intrashell core-core correlation energy, where the former involves explicit correlation of the $3d$ electrons together with the $3s$ and $3p$ electrons. Hence in the spirit of correlation consistency, the present core-valence basis sets add a $1f1g$ set to the cc-pVTZ to yield the cc-pwCVTZ set, a $1f1g1h$ set to the cc-pVQZ to make the cc-pwCVQZ basis,

TABLE II. Atomic nonrelativistic Hartree-Fock energies for the lowest $4s^23d^{m-2}$ and $4s^13d^{m-1}$ states with comparison to accurate numerical results.

Atom	State	cc-pVTZ	cc-pVQZ	cc-pV5Z	Numerical ^a
Sc	$4s^23d^1, ^2D$	-759.735 450	-759.735 684	-759.735 714	-759.735 718
	$4s^13d^2, ^4F$	-759.698 427	-759.698 739	-759.698 781	-759.698 786
Ti	$4s^23d^2, ^3F$	-848.405 611	-848.405 958	-848.405 992	-848.405 997
	$4s^13d^3, ^5F$	-848.385 685	-848.386 103	-848.386 148	-848.386 154
V	$4s^23d^3, ^4F$	-942.883 834	-942.884 293	-942.884 331	-942.884 338
	$4s^13d^4, ^6D$	-942.879 201	-942.879 728	-942.879 776	-942.879 783
Cr	$4s^23d^4, ^5D$	-1043.309 071	-1043.309 751	-1043.309 811	-1043.309 82
	$4s^13d^5, ^7S$	-1043.355 682	-1043.356 320	-1043.356 368	-1043.356 38
Mn	$4s^23d^5, ^6S$	-1149.865 370	-1149.866 189	-1149.866 242	-1149.866 25
	$4s^13d^6, ^6D$	-1149.742 990	-1149.743 884	-1149.743 947	-1149.743 96
Fe	$4s^23d^6, ^5D$	-1262.442 562	-1262.443 594	-1262.443 654	-1262.443 67
	$4s^13d^7, ^5F$	-1262.376 411	-1262.377 529	-1262.377 604	-1262.377 62
Co	$4s^23d^7, ^4F$	-1381.413 197	-1381.414 471	-1381.414 538	-1381.414 55
	$4s^13d^8, ^4F$	-1381.356 914	-1381.358 282	-1381.358 368	-1381.358 38
Ni	$4s^23d^8, ^3F$	-1506.869 252	-1506.870 812	-1506.870 890	-1506.870 91
	$4s^13d^9, ^3D$	-1506.822 293	-1506.823 908	-1506.824 009	-1506.824 03
Cu	$4s^23d^9, ^2D$	-1638.948 666	-1638.949 992	-1638.950 068	-1638.950 08
	$4s^13d^{10}, ^2S$	-1638.961 926	-1638.963 614	-1638.963 725	-1638.963 74
Zn	$4s^23d^{10}, ^1S$	-1777.846 655	-1777.848 025	-1777.848 104	-1777.848 12
	$4s^13d^{10}4p^1, ^3P$	-1777.749 331	-1777.750 848	-1777.750 955	-1777.751 00

^aReference 31.

and a $1f1g1h1i$ set to the cc-pV5Z basis to construct a cc-pwCV5Z basis. Of course, the problem of overlapping functions must still be addressed. In the present work, in order not to degrade the description of the valence space, the outermost functions from the valence sets were fixed and the remaining $fghi$ correlating functions were reoptimized. This is similar to the prescription used by Bauschlicher, Jr. for his indium core-valence basis set.³⁰ In the present case, these functions were reoptimized using the sum of the weighted core-valence correlation energy (cf., Ref. 8) and the average valence-only CISD energy of up to three atomic states (as discussed above for the valence basis sets).

Lastly, additional spd functions appropriate for $3s3p$ correlation were added to obtain the final cc-pwCVnZ basis sets. In each case a set of $2s2p2d$ functions optimized for the weighted core-valence correlation energy was added to each basis set, TZ through 5Z. Based on studies of the incremental core-valence correlation energy in both Ti and Ni, larger spd correlating sets were not deemed necessary since further spd functions recovered much less than the $fghi$ functions that were also added as discussed above. Hence the final cc-pwCVnZ basis sets consisted of $[9s8p6d3f2g]$ for cc-pwCVTZ(-DK), $[10s9p7d4f3g2h]$ for cc-pwCVQZ(-DK), and $[11s10p8d5f4g3h2i]$ for cc-pwCV5Z(-DK).

C. Diffuse function augmented sets, aug-cc-pVnZ

Finally, in order provide an accurate description of both anionic character and weak interactions, extra diffuse functions should be added to each basis set, either cc-pVnZ or cc-pwCVnZ. In the correlation consistent basis sets for the p -block elements, additional diffuse functions were added for each angular momentum function present in the regular set, e.g., one additional s , p , d , and f function was added to the cc-pVTZ basis set to form the aug-cc-pVTZ set. In these

cases the exponents of these additional diffuse functions were obtained through optimizations on the atomic negative ions. In principle, a similar prescription could also be followed in the present case for the transition metal elements, and in fact this was the procedure initially used in this work. The problem, however, was that for many of the transition metal elements the atomic electron affinity is very small, often only greater than zero with very large basis sets and extensive electron correlation. This tended to result in diffuse exponents that were seemingly much too small for use in most molecular environments. A simple alternative scheme is to just extend the most diffuse part of the existing basis sets in an even-tempered fashion. Comparison of the outer two exponents in both the cc-pVnZ and cc-pwCVnZ basis sets suggested that the most consistent set of diffuse functions was obtained by carrying out an even-tempered extension of the two most diffuse exponents in the cc-pwCVnZ basis sets. This strategy was followed in each case to obtain aug-cc-pVnZ and aug-cc-pVnZ-DK basis sets with $n=T, Q$, and 5 (of course, these same diffuse functions can also be used to generate aug-cc-pwCVnZ and aug-cc-pwCVnZ-DK basis sets).

III. BENCHMARK CALCULATIONS

A. Atomic properties

Nonrelativistic HF total energies calculated with the cc-pVnZ ($n=T, Q, 5$) basis sets are shown in Table II for the two lowest electronic states of Sc–Zn, where they are also compared to the accurate numerical results of Tatewaki and Koga.³¹ The HF errors are observed to be very balanced between the ground and excited states, and range from a maximum of 1.8 mE_h for the triple- ζ set to 45 μE_h for the 5- ζ set. The results for the ground states of the cations and

TABLE III. Calculated CCSD(T) $4s^23d^{m-2} \rightarrow 4s^13d^{m-1}$ excitation energies (kcal/mol) for valence $4s3d$ correlation. (b) Calculated effects of $3s3p$ electron correlation, ΔCV , (kcal/mol) on the $4s^23d^{m-2} \rightarrow 4s^13d^{m-1}$ valence-only excitation energies at the CCSD(T)-DK level of theory ($\Delta CV=3s3p3d4s$ value $-3d4s$ value; both calculations in the same core-valence basis set).

Basis	Sc	Ti	V	Cr	Mn	Fe	Co	Ni	Cu
(a)					Nonrelativistic				
cc-pVTZ	37.30	21.73	7.35	-25.51	55.97	23.41	10.93	-1.04	-38.17
cc-pVQZ	36.98	21.24	6.78	-25.73	53.55	21.07	8.41	-3.84	-41.33
cc-pV5Z	36.94	21.16	6.67	-25.75	52.46	20.00	7.36	-4.97	-42.40
CBS-NR ^a	36.91	21.09	6.58	-25.77	51.57	19.13	6.50	-5.88	-43.27
					DK relativistic				
cc-pVTZ-DK	39.99	25.02	11.27	-20.74	60.55	29.29	18.31	6.98	-28.46
cc-pVQZ-DK	39.68	24.54	10.71	-20.91	58.15	26.96	15.39	4.28	-31.64
cc-pV5Z-DK	39.63	24.46	10.61	-20.92	57.07	25.91	14.35	3.18	-32.68
CBS-DK(TQ) ^b	39.46	24.18	10.31	-21.04	56.40	25.26	13.25	2.31	-33.95
CBS-DK ^a	39.60	24.39	10.52	-20.93	56.19	25.05	13.51	2.28	-33.54
Expt. ^c	32.91	18.58	5.65	-23.13	49.47	20.18	9.62	-0.69	-34.37
(b)					DK relativistic				
cc-pwCVTZ-DK	-4.71	-4.15	-3.51	-0.83	-4.65	-2.84	-2.10	-1.34	0.53
cc-pwCVQZ-DK	-5.86	-5.06	-4.30	-1.68	-5.33	-3.64	-2.79	-1.99	-0.13
cc-pwCV5Z-DK	-6.29	-5.40	-4.63	-2.06	-5.68	-4.03	-3.17	-2.39	-0.55
CBS-DK(TQ) ^b	-6.71	-5.72	-4.87	-2.31	-5.83	-4.22	-3.29	-2.48	-0.62
CBS-DK ^a	-6.63	-5.69	-4.91	-2.36	-5.97	-4.35	-3.48	-2.71	-0.88

^aBest estimate calculated as the averaged extrapolated value from using the TZ-5Z sets with Eq. (1) and QZ-5Z sets with Eq. (2).

^bObtained using the TZ and QZ basis sets with Eq. (2).

^cFrom Ref. 49. Spin-orbit effects have been removed from these values using the experimental fine-structure splittings.

anions (not shown) are very similar (utilizing the numerical HF results of Ref. 32). However, the HF energies for the anions with the aug-cc-pV5Z basis sets are uniformly 0.2 mE_h too high. With the exception of Cu, however, which has only a very small NR-HF electron affinity, all of the other atomic negative ions are unstable with respect to loss of an electron at the HF level of theory, and these residual errors are essentially eliminated by adding an additional shell of even-tempered diffuse functions, i.e., d-aug-cc-pVnZ. Hence the HF errors with the aug-cc-pV5Z basis sets are mainly reflective of the difficulty in describing the atomic anions at the HF level. It should also be noted that the relativistic DK-HF energy differences between the triple- ζ and 5- ζ sets (using the cc-pVnZ-DK or aug-cc-pVnZ-DK basis sets) are comparable to the nonrelativistic results in every case.

Excitation energies ($4s^23d^{m-2} \rightarrow 4s^13d^{m-1}$), ionization potentials, and electron affinities calculated at the coupled cluster singles and doubles level of theory with perturbative triples, CCSD(T),³³ both nonrelativistic and relativistic, are shown in Tables III–V, respectively, as a function of the basis set. The open-shell variant of CCSD(T) used in this work utilized restricted open-shell HF (ROHF) orbitals (state-averaged ROHF in this case for symmetry equivalencing), but allowed for small amounts of spin contamination in the solution of the CCSD equations, i.e., R/UCCSD(T).³⁴ Complete basis set limits have also been estimated in each case by extrapolation of the total energies via both a mixed exponential and Gaussian form,³⁵

$$E_n = E_{\text{CBS}} + Ae^{-(n-1)} + Be^{-(n-1)^2}, \quad (1)$$

and a two-point ℓ^{-3} formula,³⁶

$$E_n = E_{\text{CBS}} + \frac{A}{n^3}. \quad (2)$$

The best estimate CBS limits shown in the tables and figures of this work correspond to the average of these two results using TZ, QZ, and 5Z basis sets for Eq. (1) and QZ and 5Z for Eq. (2). CBS extrapolations that involve using just the TZ and QZ basis sets with Eq. (2) are also given for the DK results. In addition, the experimental results shown have been adjusted for spin-orbit coupling effects, which have not been included in the current *ab initio* results, and reflect the *j*-averaged values using the experimental splittings. Note that in the case of Ni, the lowest spin-orbit coupled state arises from the $4s^23d^8(^3F)$ configuration, yet the lowest energy *j*-averaged state corresponds to the $4s^13d^9(^3D)$ configuration. The former has been used as the reference for the neutral ground state in both the ionization potential and electron affinity of Ni atom in this work. The overall relative shift in energy between the two states produced by *j* averaging is 1.27 kcal/mol.

1. Atomic excitation energies

Focusing first on the CCSD(T) excitation energies with only valence electron correlation included [Table III(a)], in every case the convergence with respect to basis set is from above, i.e., increases in the basis set stabilize the $4s^13d^{m-1}$ states. In general the convergence towards the CBS limit is regular and rapid. In particular for the early transition metals, Sc–Cr, the TZ results are already within a few tenths of a kcal/mol of the CBS limits, while for Mn–Cu the TZ basis-set results are within about 5 kcal/mol. The effects of scalar relativity on the excitation energies, determined as the differ-

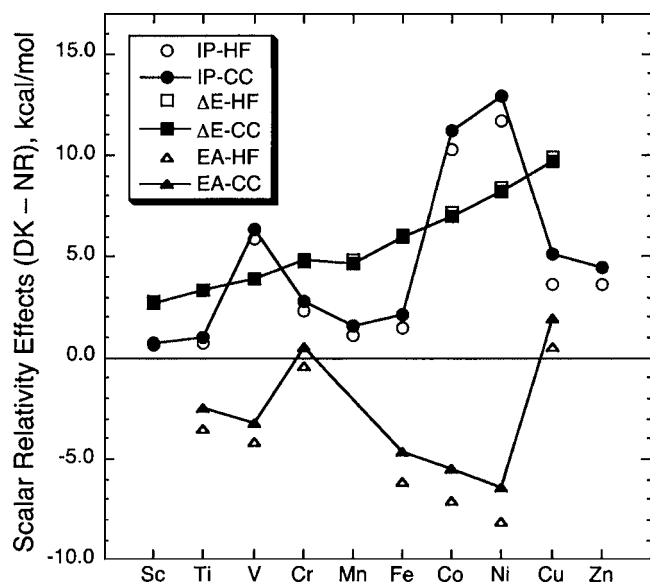


FIG. 2. Complete basis set limits for the effects of scalar relativity on the HF and CCSD(T) atomic ionization potentials (IPs), $4s^2 \rightarrow 4s^1$ excitation energies (ΔE), and electron affinities (EAs).

ence between the NR-CCSD(T)/cc-pVnZ and DK-CCSD(T)/cc-pVnZ-DK results, can be extracted from Table III(a), and the CBS differences are plotted in Fig. 2. In general the basis set dependence of the scalar relativistic effect is nearly converged in these cases already at the TZ level, and the magnitude of the effect, which ranges from just under 3 kcal/mol for Sc to nearly 10 kcal/mol for Cu, increases very regularly as a function of the atomic number, as shown in Fig. 2, and always increases the excitation energy. These latter trends are expected since scalar relativistic effects should approximately increase as Z^2 with a strong stabilization of the $4s$ orbital and a concomitant destabilization of the $3d$. These excitation energies all involve a $4s^2 3d^{m-2} \rightarrow 4s^1 3d^{m-1}$ excitation. In fact the trend shown in Fig. 2 does closely follow a Z^2 dependence, but only if the early metals (Sc–Cr) are analyzed separately from the later ones (Mn–Cu). As also shown in Fig. 2, scalar relativistic effects calculated at the HF level of theory are nearly identical to the CCSD(T) values for these excitation energies, with a maximum correlation effect of just 0.23 kcal/mol for the Ni atom.

Upon comparing the valence correlated results to experiment in Table III(a), it can be observed that the inclusion of scalar relativity actually worsens the agreement with experiment once the basis set is extrapolated to the CBS limit. Of course it is well known that $3s3p$ correlation can be very important for the transition metal elements, and the contributions to the excitation energies from this effect using the cc-pwCVnZ-DK basis sets are given in Table III(b) and plotted in Fig. 3. The nonrelativistic results were within 0.1 kcal/mol of the DK values and are not explicitly shown [also true for the ionization potentials (IPs) and electron affinities (EAs) discussed below]. For each element, correlation of the $3s$ and $3p$ electrons preferentially lowers the electronic state arising from the $4s^1 3d^{m-1}$ occupation, with the largest effect at the CBS limit exhibited in Sc (–6.63 kcal/mol) and the smallest in Cu (–0.88 kcal/mol).

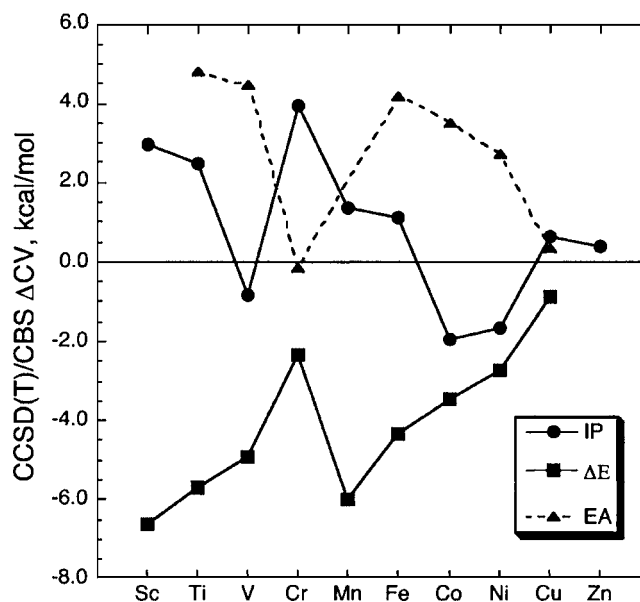


FIG. 3. Complete basis set limits for the effects of $3s3p$ electron correlation on the valence-only DK-CCSD(T) atomic ionization potentials (IPs), $4s^2 \rightarrow 4s^1$ excitation energies (ΔE s), and electron affinities (EAs).

The convergence with basis set is regular, with the cc-pwCVTZ-DK basis sets generally underestimating the total effect by up to 1.9 kcal/mol (Sc). In the case of Cu, the core-valence effect changes sign as a function of basis set, hence the TZ result is actually opposite in sign to the CBS limit value. It should be noted, however, that in each case a two-point extrapolation via Eq. (2) using just the TZ and QZ basis sets yields a very accurate estimate of the CBS limit, with the largest differences being just 0.2–0.3 kcal/mol (Co–Cu). Qualitatively it can be observed in Fig. 3 that the magnitude of the effect decreases as the number of $3d$ electrons increase, but two separate trends are apparent between the early transition metals, Sc–Cr, and those with at least a half-full d shell, Mn–Cu. In fact the $3s3p$ correlation effect on ΔE is nearly as large for Mn as in Sc. The final DK-CCSD(T)/CBS results including $3s3p$ correlation are shown in Table VI where they are compared to experiment. As can also be observed in Fig. 4 where the differences between these theoretical values and experiment are plotted, all errors are under 1 kcal/mol and only in the case of Mn is the difference greater than 0.5 kcal/mol. Interestingly, the differences between theory and experiment also exhibit two different trends between the early and late transition metals, which presumably reflects errors intrinsic to the CCSD(T) method for this property.

Our results above for Ti and Fe can be directly compared to the previous CCSD(T) calculations of Ricca and Bauschlicher¹² and Bauschlicher¹⁴ who used their own correlation-consistent-style basis sets. In the case of Ti, our nonrelativistic, valence-only results are nearly identical (within 0.1 kcal/mol) to the excitation energies of Ref. 14. This is not surprising since these basis sets have much in common. In the case of the $3s3p$ correlation treatment, however, the core-valence correlation effect calculated with the cc-pwCVnZ basis sets of the present work tends to yield somewhat faster convergence towards the CBS limit, and the

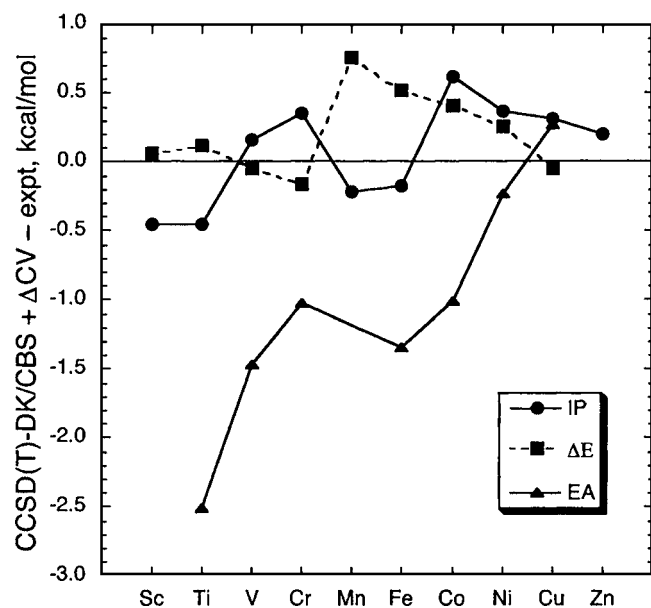


FIG. 4. A comparison of experiment vs DK-CCSD(T)/CBS+3s3p results for the atomic IPs, ΔE s, and EAs.

NR limit obtained in the present work, -5.82 kcal/mol, is smaller in magnitude from that of Bauschlicher by about 0.5 kcal/mol. As discussed below for TiH, however, much of this can be attributed to the choice of orbitals in Ref. 14 and not to deficiencies in the basis set. Somewhat larger differences are observed between the present work and results obtained with the Fe basis sets of Ricca and Bauschlicher¹² particularly for their valence sets. In this case the nonrelativistic, valence correlation separations of the present work are consistently higher by about 1.5 kcal/mol, which persists to

the estimated CBS limits. Comparison of the results that include $3s3p$ correlation, however, only differ by about 0.5 kcal/mol. The only difference in the basis set of Ricca and Bauschlicher in the $3s3p$ case compared to the valence-only calculation was a slightly different contraction of the primitive s set. Indeed, use of this latter basis set for valence-only correlation yields an Fe $^5F-^5D$ separation nearly identical to the values calculated in the present work. This suggests that the valence basis set of Ref. 12 perhaps does not provide enough s -type correlating functions to avoid slightly biasing the calculation against the $4s^2(^5D)$ ground state.

2. Atomic ionization potentials

CCSD(T) ionization potentials for $4s3d$ correlation are displayed in Table IV(a) together with their experimental values. For Sc–V very little basis set dependence is observed, with differences between cc-pVTZ and the CBS limit of only 0.4 – 0.7 kcal/mol. The corresponding ranges for the remaining elements vary from only 0.2 kcal/mol in Ni to about 5.7 kcal/mol in Cu. Calculations with the aug-cc-pVnZ basis sets demonstrated that the somewhat slower convergence for Cu and also Zn was due to the lack of a sufficiently diffuse f -type function for the smaller sets. Note that this trend is not present at the HF level and is presumably due to important sd correlation effects.^{37,38} Faster convergence with the aug-cc-pVnZ basis sets was also observed for the excitation energies discussed above and can be attributed to the same effect. Basis set extrapolation, however, with either the cc-pVnZ or aug-cc-pVnZ basis sets still yielded essentially the same CBS limits for the IPs of Cu and Zn. In the case of the IPs, scalar relativity is observed to increase their values above the nonrelativistic IPs since the electron is

TABLE IV. (a) Calculated CCSD(T) ionization potentials (kcal/mol) for valence $4s3d$ correlation. (b) Calculated effects of $3s3p$ electron correlation (kcal/mol), ΔCV , on the valence-only ionization potentials at the CCSD(T)-DK level of theory ($\Delta CV=3s3p3d4s$ value– $3d4s$ value; both calculations in the same core-valence basis set).

Basis	Sc	Ti	V	Cr	Mn	Fe	Co	Ni	Cu	Zn
(a)	Nonrelativistic									
cc-pVTZ	146.82	152.80	149.45	147.88	166.00	176.25	173.34	164.46	167.02	208.03
cc-pVQZ	146.98	153.20	149.65	149.00	167.24	177.61	172.87	163.95	170.07	209.85
cc-pV5Z	147.09	153.39	149.82	149.35	167.80	178.29	172.87	164.13	171.55	211.00
CBS-NR ^a	147.18	153.54	149.95	149.63	168.25	178.84	172.86	164.27	172.75	211.94
	DK relativistic									
cc-pVTZ-DK	147.57	153.78	155.75	150.66	167.54	178.35	184.55	177.20	171.95	212.40
cc-pVQZ-DK	147.73	154.17	155.96	151.80	168.81	179.73	184.01	176.76	175.12	214.32
cc-pV5Z-DK	147.83	154.36	156.13	152.15	169.38	180.42	184.03	176.96	176.63	215.49
CBS-DK(TQ) ^b	147.85	154.46	156.12	152.63	169.74	180.74	183.61	176.44	177.43	215.71
CBS-DK ^a	147.91	154.52	156.27	152.44	169.84	180.99	184.05	177.13	177.86	216.44
Expt. ^c	151.32	157.47	155.25	156.04	171.43	182.27	181.47	175.12	178.17	216.63
(b)	DK relativistic									
cc-pwCVTZ-DK	2.92	2.47	0.88	4.17	1.20	0.96	-0.35	-0.18	0.67	0.25
cc-pwCVQZ-DK	2.94	2.47	-0.11	4.04	1.31	1.05	-1.22	-0.91	0.64	0.32
cc-pwCV5Z-DK	2.95	2.48	-0.52	3.99	1.34	1.08	-1.63	-1.31	0.63	0.36
CBS-DK(TQ) ^b	2.95	2.47	-0.83	3.95	1.38	1.12	-1.85	-1.45	0.61	0.37
CBS-DK ^a	2.97	2.49	-0.86	3.95	1.37	1.11	-1.96	-1.64	0.62	0.39

^aBest estimate calculated as the averaged extrapolated value from using the TZ-5Z sets with Eq. (1) and QZ-5Z sets with Eq. (2).

^bObtained using the TZ and QZ basis sets with Eq. (2).

^cSpin-orbit effects have been removed from these values using the experimental fine-structure splittings. See also the footnote to Table VI.

TABLE V. (a) Calculated CCSD(T) electron affinities (kcal/mol) for valence $4s3d$ correlation. (b) Calculated effects of $3s3p$ electron correlation, ΔCV , on the valence-only electron affinities (kcal/mol) at the CCSD(T)-DK level of theory ($\Delta CV=3s3p3d4s$ value– $3d4s$ value; both calculations in the same core-valence basis set).

Basis	Ti	V	Cr	Fe	Co	Ni	Cu
(a)							
Nonrelativistic							
aug-cc-pVTZ	–3.38	8.85	13.57	–1.23	13.35	27.68	25.26
aug-cc-pVQZ	–2.96	9.48	13.92	0.70	15.34	29.84	25.96
aug-cc-pV5Z	–2.85	9.64	14.05	1.55	16.11	30.59	26.25
CBS-NR ^a	–2.76	9.77	14.16	2.24	16.74	31.20	26.48
DK relativistic							
aug-cc-pVTZ-DK	–5.85	5.62	14.11	–5.80	7.85	21.34	27.15
aug-cc-pVQZ-DK	–5.43	6.23	14.46	–3.89	9.84	23.44	27.91
aug-cc-pV5Z-DK	–5.33	6.39	14.60	–3.06	10.61	24.19	28.20
CBS-DK(TQ) ^b	–5.13	6.68	14.72	–2.50	11.30	24.97	28.46
CBS-DK ^a	–5.24	6.52	14.71	–2.38	11.24	24.80	28.44
Expt. ^c	2.09	12.45	15.59	3.13	15.71	27.76	28.50
(b)							
DK relativistic							
aug-cc-pwCVTZ-DK	3.61	3.32	–0.01	3.17	2.59	1.89	0.40
aug-cc-pwCVQZ-DK	4.31	3.95	–0.08	3.62	2.96	2.26	0.32
aug-cc-pwCV5Z-DK	4.59	4.24	–0.12	3.92	3.24	2.52	0.33
CBS-DK(TQ) ^b	4.83	4.41	–0.14	3.95	3.22	2.52	0.27
CBS-DK ^a	4.81	4.47	–0.15	4.17	3.47	2.74	0.33

^aBest estimate calculated as the averaged extrapolated value from using the TZ-5Z sets with Eq. (1) and QZ-5Z sets with Eq. (2).

^bObtained using the TZ and QZ basis sets with Eq. (2).

^cReference 50. Spin-orbit effects have been removed from these values using the experimental fine-structure splittings.

removed from the $4s$ orbital. This tends to result in better agreement with the experimental values at the CCSD(T) level of theory. The differences between the CBS-NR and CBS-DK values are plotted in Fig. 2, where the result of differing $4s$ occupations can be plainly observed. The largest scalar relativity effects are calculated for V, Co, and Ni where the ionization involves a $4s^2$ to $4s^0$ change, while smaller effects are observed in Sc, Ti, Mn, Fe, and Zn where the cation state has a $4s^1$ occupation. The remaining two elements, Cr and Cu, are the only elements where the electron is ionized from a singly occupied $4s$. It should be noted that the DK-HF scalar relativity corrections from this work are within 0.1–0.2 kcal/mol of the accurate numerical DHF values of Koga *et al.*³⁹ In contrast to the excitation energies, the impact of electron correlation on the scalar relativistic correction is relatively large, rising to 1.5 kcal/mol for the Cu atom.

From the comparison between the CBS-DK values and experiment in Table IV(a), it might be inferred that outer-core correlation has a significant effect on these atomic IPs. As shown in Table IV(b), $3s3p$ correlation affects the IPs from about 0.4 to nearly 4 kcal/mol. For most of the elements, the core-valence (CV) effect, which is also plotted in Fig. 3, tends to increase the calculated valence correlated IPs, except for the elements that involve a change in $3d$ occupation upon ionization (V, Co, and Ni). In these cases the CV contribution is negative and exhibits a much larger basis set dependence [cf., Table IV(b)] compared to the other elements. The final CBS-DK+CV ionization potentials are compared to experiment in Table VI and the errors are plot-

ted in Fig. 4. All of the differences between theory and experiment are now within 1 kcal/mol, with the largest errors observed for the later transition metals.

3. Atomic electron affinities

The most challenging atomic property considered in the present work is the electron affinity, since, with the exception of the Cu atom, electrons are bound purely by electron correlation effects in these elements. The present CCSD(T) valence $4s3d$ correlated results are shown in Table V(a), while the CV effects are given in Table V(b). The aug-cc-pVnZ basis sets were used in all cases. The Sc[–] anion has a $^1D(4s^13d^24p^1)$ ground state, which is not well described by single determinant methods such as CCSD(T) and has not been included in the present study. In addition, since the Mn and Zn atoms do not bind electrons, they are also not treated. Among the remaining elements, all except Cr and Cu involve electron attachment into a $3d$ orbital. The $4s^1$ ground states of Cr and Cu yield $4s^2$ ground states for their anions. As shown in Table V(a) and Fig. 2, scalar relativity generally decreases the electron affinity due to destabilization of the $3d$ orbital, except for Cr and Cu where, of course, it leads to an increase (the $4s$ is stabilized). Hence, in most cases the inclusion of scalar relativity results in CCSD(T) electron affinities further from the experimental EAs in comparison to the nonrelativistic values, since the CCSD(T) method tends to underestimate full configuration interaction (FCI) electron affinities. As also shown in Fig. 2, HF calculations of the scalar relativity effect on the electron affinity are not particu-

TABLE VI. Summary of relativistic DK-CCSD(T)/CBS excitation energies, ionization potentials, and electron affinities calculated with $3s3p3d4s$ electron correlation compared to experiment (kcal/mol). Spin-orbit coupling effects have been removed from the experimental values using the experimental fine-structure splittings.

	$\Delta E(4s^2 3d^{m-2} \rightarrow 4s^1 3d^{m-1})^a$		IP		EA	
	Theory	Expt. ^b	Theory	Expt.	Theory	Expt.
Sc	32.97	32.91	150.88	151.32 ^c
Ti	18.70	18.58	157.01	157.47 ^d	-0.43	2.09 ^e
V	5.61	5.65	155.41	155.25 ^f	10.98	12.45 ^e
Cr	-23.29	-23.13	156.39	156.04 ^c	14.56	15.59 ^g
Mn	50.23	49.47	171.21	171.43 ^c
Fe	20.69	20.18	182.10	182.27 ^h	1.79	3.13 ⁱ
Co	9.99	9.62	182.04	181.47 ^h	14.71	15.71 ^j
Ni ^k	-0.43	-0.69	175.49	175.12 ^h	27.54	27.76 ^j
Cu	-34.27	-34.37	178.48	178.17 ^l	28.77	28.50 ^g
Zn	94.10	93.48	216.83	216.63 ^m

^a $4s^2 3d^{10} \rightarrow 4s^1 3d^{10} 4p^1$ for Zn.

^bReference 49.

^cReference 51.

^dReference 52.

^eReferences 50, 57, and 58.

^fReference 53.

^gReference 59.

^hReference 54.

ⁱReference 60 with fine-structure data for Fe⁻ from Ref. 57.

^jReference 61 with some fine-structure data for Co⁻ from Ref. 57.

^kThe IPs and EAs are shown relative to the j -averaged $4s^2 3d^8(^3F)$ state.

^lReference 55.

^mReference 56.

larly accurate compared to CCSD(T), which reflects the importance of dynamic electron correlation for the EAs of the $3d$ transition metals. Hence while our DK-HF scalar relativity corrections are within 0.1-0.3 kcal/mol of the numerical DHF values of Koga *et al.*,³⁹ electron correlation adds nearly 1–2 kcal/mol to the HF values (decreasing the magnitude of the negative HF contributions and increasing the magnitude of the positive HF contributions). Last, it should be noted that the convergence with basis set of the EAs shown in Table V(a) is regular and relatively rapid; however, at the NR-CCSD(T)/CBS or DK-CCSD(T)/CBS-DK levels, the electron affinity of Ti is still strongly negative when only valence electrons are correlated.

Core-valence correlation effects on the calculated electron affinities are shown in Table V(b) for the DK relativistic calculations and these are also plotted in Fig. 3. The CV effects are large for the elements that involve electron attachment into the $3d$ orbital, ranging from nearly 5 kcal/mol for Ti to just under 3 kcal/mol for Ni. The CV effects for Cr and Cu are nearly negligible at -0.15 and 0.33 kcal/mol at the CBS-DK limit, respectively ($4s^1 \rightarrow 4s^2$ processes). The convergence with the basis set of the $3s3p$ core-valence correlation effect is relatively rapid in each case with the aug-cc-pwCVnZ basis sets. The final DK-CCSD(T)/CBS electron affinities are compared to experiment in Table VI and the (theory–experiment) differences are plotted in Fig. 4. The electron affinity of Ti is still strongly underestimated by CCSD(T), and many of the other elements also exhibit errors with respect to experiment greater than 1 kcal/mol. The electron affinities of both Ni and Cu, however, appear to be very accurately described by this level of theory. It should be

emphasized that these final differences with experiment reflect the intrinsic accuracy of CCSD(T) for this property; calculations at the CCSDT and CCSDTQ levels are currently being completed that confirm the large effects of iterative triples and quadruple excitations. Benchmark results at these levels of theory for all the atomic properties of the present paper will be presented in a subsequent paper.⁴⁰

Our calculated electron affinities can be compared to the recent CCSD(T) work of Bauschlicher and Gutsev.⁴¹ Their results using ANO-style basis sets for Ti, V, Fe, and Co compare well to our aug-cc-pVTZ-DK values. Some of the most accurate correlated calculations of excitation energies, ionization potentials, and electron affinities of the early transition metals (Sc–Mn) have recently been reported by Miura *et al.*⁴² and Osanai *et al.*⁴³ These studies used large Slater-type basis sets with multireference CI (MRCI) wave functions and included a careful treatment of both valence and core correlation effects, as well as relativity. Upon comparison of their MRCI results with the CCSD(T) values of the present study, however, it would appear that the core correlation contributions of Refs. 42 and 43 are often strongly overestimated, perhaps due to size extensivity problems with their method. This seems to be particularly apparent in the case of the EA of Ti, where the MRCI core correlation contribution (core-valence+core-core) of 8.7 kcal/mol can be compared to our CCSD(T) result of 4.8 kcal/mol. In addition, in several cases their calculated relativistic effects were often quite different from the present results, by as much as 1 kcal/mol. While it is difficult to unambiguously compare the two sets of results, it is the case that if one uses their accurate valence-only correlation results (which included extrapolations to the full

CI limit) for the ΔE_s , IPs, and EAs and then add the CCSD(T) scalar relativistic and CV corrections from the present work, the agreement with experiment is better than their reported final values in every case (the IP of Sc was unchanged). In the instances where their original disagreement was relatively large, e.g., the EA of V, which differed from experiment by 2.5 kcal/mol, the prescription above decreased this error to just 0.2 kcal/mol.

B. Molecular spectroscopic properties

Spectroscopic properties calculated at the CCSD(T) level of theory with the basis sets of the present work are given in Tables VII–XI for the electronic ground states of TiH, MnH, CuH, TiF, and Cu₂, respectively. In each case near-equilibrium potential energy curves were obtained by fitting seven energies to fifth- or sixth-degree polynomials in displacement coordinates and then employing the resulting derivatives in the usual Dunham analysis.⁴⁴ The dissociation energies were calculated relative to atomic asymptotes that were fully symmetry equivalenced. In addition, for the two species with $^4\Phi$ ground states (TiH, TiF), the HF orbitals were also symmetry equivalenced in state-averaged HF calculations. In the cases of valence-only electron correlation, both nonrelativistic calculations, which used the series of cc-pVnZ basis sets, and DK relativistic calculations, which used the series of cc-pVnZ-DK basis sets, were carried out, and the difference between the derived spectroscopic constants represented the effects of scalar relativity. The effects of core-valence correlation, i.e., the addition of the $3s3p$ electrons of the transition metal to the correlation treatment, as well as the $1s$ electrons of F in TiF, were obtained at the DK-CCSD(T) level of theory with both the valence cc-pVnZ-DK and core-valence cc-pwCVnZ-DK series of basis sets. The effects of core-valence correlation were determined as the difference between calculations with only valence electrons correlated and those with outer-core electrons included, both in the same basis set. Diffuse function augmented sets were always used on fluorine in the TiF calculations. Complete basis set limits were obtained via Eqs. (1) and (2) with the average of these two results representing the best estimate. Calculations were also carried out using the diffuse augmented analogs of each of these basis sets (aug-cc-pVnZ, etc.), but these results are only shown for Cu₂ (Table XI), which was the only case that displayed a significant difference. Finally, most of these molecules have been extensively studied in the past (see Refs. 13, 14, 37, 45, and 46) but since the focus of this work is on the basis set dependence of the various spectroscopic constants at the CCSD(T) level of theory, detailed comparisons with all of these past results are outside the scope of this study.

1. TiH, MnH, and CuH

The calculated results for the hydrides considered in this work, which were chosen since they are relatively well described by single determinant methods, are shown in Tables VII–IX. In the case of TiH (Table VII), the convergence with the basis set of the valence-only, nonrelativistic spectroscopic constants is very rapid with little variance between

TABLE VII. Summary of $X^4\Phi$ TiH CCSD(T) spectroscopic constants.

Basis set	r_e (Å)	ω_e (cm ⁻¹)	D_e (kcal/mol)
Nonrelativistic, valence correlation			
cc-pVTZ	1.8096	1514.1	48.79
cc-pVQZ	1.8086	1508.6	49.70
cc-pV5Z	1.8084	1514.1	49.97
CBS-val	1.8082	1518.5	50.19
Scalar relativistic effects, [DK-CCSD(T)]-[NR-CCSD(T)]			
cc-pVTZ-(DK,NR)	0.0002	-5.1	-1.05
cc-pVQZ-(DK,NR)	0.0002	-1.2	-1.06
cc-pV5Z-(DK,NR)	0.0003	0.0	-1.06
CBS-rel	0.0004	1.0	-1.07
DK relativistic, Ti $3s3p$ correlation effects (CV-valence)			
cc-pVTZ-DK	-0.0337	38.5	0.11
cc-pVQZ-DK	-0.0342	44.5	0.50
cc-pV5Z-DK	-0.0362	41.7	0.64
CBS-CV1	-0.0379	39.6	0.76
cc-pwCVTZ-DK	-0.0301	35.2	-0.09
cc-pwCVQZ-DK	-0.0328	46.7	0.24
cc-pwCV5Z-DK	-0.0337	38.7	0.36
CBS-CV2	-0.0344	31.8	0.47
Total, CBS(val+rel+CV2)	1.7742	1551.3	49.6
Expt. ^a	1.779		50.2±2.1

^aThe experimental structure corresponds to an r_0 value from Ref. 62. D_e was derived from Ref. 63 with 298 K thermal corrections to 0 K from Ref. 14. The *ab initio* ω_e value from this work was used to derive D_e .

triple- ζ and the CBS limit. It should be noted that at this level, the CCSD(T) bond length is longer than experiment by more than 0.02 Å, while the equilibrium dissociation energy is nearly identical to the experimental value. As also shown in Table VII, however, while scalar relativity has nearly no effect on r_e and ω_e , the dissociation energy is lowered by just over 1 kcal/mol. The effects of scalar relativity are also well described with just the cc-pVTZ basis sets. Not unexpectedly, correlation of the $3s3p$ electrons of Ti has a strong impact on the spectroscopic constants. Regular convergence with basis set is observed with both the cc-pVnZ-DK and cc-pwCVnZ-DK basis sets; however, use of the former seems to overestimate the total CV effects. At the CBS limit, core-valence correlation is calculated to decrease the valence-only r_e value by 0.034 Å and the harmonic frequency increases by 32 cm⁻¹. The dissociation energy, however, is increased by just 0.5 kcal/mol. The final $3s3p$ correlated DK-CCSD(T)/CBS results are in good agreement with experiment, with the *ab initio* r_e value being slightly smaller than the experimental r_0 . Our results for TiH can be directly compared to the CCSD(T) results of Bauschlicher¹⁴ using his cc-pVnZ basis sets ($n=T, Q, 5$). All of the results are nearly identical as expected, except for the core-valence correlation effect on D_e where a large +1.4 kcal/mol contribution was reported in Ref. 14 compared to our result of +0.5 kcal/mol. The origin of this difference, however, resides partly in the valence-only results where the D_e of Ref. 14 was about 0.5 kcal/mol smaller than that of the present work. After carrying out additional calculations in our laboratory using the basis sets of Ref. 14, however, it was apparent that the smaller D_e was not a basis set effect at all but

TABLE VIII. Summary of $X^7\Sigma^+$ MnH CCSD(T) spectroscopic constants.

Basis set	r_e (Å)	ω_e (cm ⁻¹)	D_e (kcal/mol)
Nonrelativistic, valence correlation			
cc-pVTZ	1.7432	1549.9	38.80
cc-pVQZ	1.7430	1546.0	39.34
cc-pV5Z	1.7431	1543.3	39.50
CBS-val	1.7432	1541.0	39.64
Scalar relativistic effects, [DK-CCSD(T)]-[NR-CCSD(T)]			
cc-pVTZ-(DK,NR)	-0.0059	5.2	-0.85
cc-pVQZ-(DK,NR)	-0.0059	5.8	-0.88
cc-pV5Z-(DK,NR)	-0.0059	5.8	-0.89
CBS-rel	-0.0059	5.8	-0.90
DK relativistic, Mn 3s3p correlation effects (CV=valence)			
cc-pVTZ-DK	-0.0097	3.4	-0.37
cc-pVQZ-DK	-0.0122	19.2	-0.29
cc-pV5Z-DK	-0.0108	8.8	-0.36
CBS-CV1	-0.0096	0.3	-0.42
cc-pwCVTZ-DK	-0.0081	5.0	-0.67
cc-pwCVQZ-DK	-0.0085	6.2	-0.64
cc-pwCV5Z-DK	-0.0089	7.1	-0.63
CBS-CV2	-0.0091	7.8	-0.62
Total, CBS(val+rel+CV2)	1.7281	1554.6	38.1
Expt. ^a	1.7308	1546.85	31.5±4.4

^aReferences 64 and 65. The above experimental values of r_e and ω_e were used to convert the 298 K D^0 of Ref. 65, 30.2±4.4 kcal/mol, to D_e (D_0 = 29.3 kcal/mol).

was due to the use of restricted HF (RHF) orbitals in the atomic and molecular calculations that were not fully symmetry equivalenced and had small resulting symmetry contaminations from the high angular momentum functions in the 3s and 3p orbitals. Hence, the 3s3p core orbitals were slightly different in character than in the present work. This example stresses the difficulty in unambiguously comparing two sets of calculations even when they superficially appear to be nearly identical.

The results for MnH shown in Table VIII are very similar to those of TiH with very little basis set dependence calculated for the valence-only correlated, nonrelativistic spectroscopic constants. As expected, the effects of scalar relativity are stronger for MnH than those calculated for TiH, with decreases in the bond length by nearly 0.006 Å. The scalar relativity effect on D_e , -0.90 kcal/mol, is similar, however, to that of TiH. More regular convergence of the 3s3p correlation effect is obtained with the cc-pwCVnZ-DK basis sets compared to cc-pVnZ-DK; however, the CBS limits are nearly identical. The changes in r_e and ω_e with 3s3p correlation are about a factor of 4 smaller in magnitude than obtained for TiH, while the CV effect on D_e is opposite in sign but similar in magnitude. The final CCSD(T) results for MnH are in excellent agreement with experiment for r_e and ω_e , but the predicted D_e value is significantly above the experimental result, even given the latter's rather large error bars. Given the expected accuracy of the present work, the experimental dissociation energy should probably be re-evaluated.

The results for CuH shown in Table IX show well behaved convergence with basis set but with a somewhat larger

TABLE IX. Summary of $X^1\Sigma^+$ CuH CCSD(T) spectroscopic constants.

Basis Set	r_e (Å)	ω_e (cm ⁻¹)	D_e (kcal/mol)
Nonrelativistic, valence correlation			
cc-pVTZ	1.4768	1884.0	62.24
cc-pVQZ	1.4800	1878.0	62.47
cc-pV5Z	1.4816	1872.0	62.41
CBS-val	1.4829	1867.0	62.37
Scalar relativistic effects, [DK-CCSD(T)]-[NR-CCSD(T)]			
cc-pVTZ-(DK,NR)	-0.0251	85.3	2.67
cc-pVQZ-(DK,NR)	-0.0250	81.5	2.56
cc-pV5Z-(DK,NR)	-0.0250	81.6	2.54
CBS-rel	-0.0250	81.7	2.52
DK relativistic, Cu 3s3p correlation effects (CV=valence)			
cc-pVTZ-DK	-0.0021	-1.3	0.11
cc-pVQZ-DK	-0.0018	8.3	0.08
cc-pV5Z-DK	-0.0002	0.9	-0.08
CBS-CV1	0.0011	-5.2	-0.20
cc-pwCVTZ-DK	-0.0004	2.8	-0.09
cc-pwCVQZ-DK	0.0005	0.1	-0.18
cc-pwCV5Z-DK	0.0010	-1.9	-0.26
CBS-CV2	0.0014	-3.5	-0.33
Total, CBS(val+rel+CV2)	1.4594	1945.2	64.6
Expt. ^a	1.4626	1940.77	63±4

^aReferences 66 and 67. The above experimental values of r_e and ω_e were used to convert the 298 K D^0 of Ref. 67, 61±4 kcal/mol, to D_e (D_0 = 60 kcal/mol).

basis set dependence for r_e than in the cases of TiH and MnH. It is worth mentioning that the aug-cc-pVnZ results yielded essentially identical CBS limits, but the bond length converged from above. The scalar relativistic effects on r_e , ω_e , and D_e are all substantial, -0.025 Å, 82 cm⁻¹, and 2.5 kcal/mol, respectively, at the CBS limit. Note that in contrast to TiH and MnH, relativistic effects strongly stabilize the bond in CuH. As discussed in detail by Bauschlicher *et al.*,³⁸ this is presumably due to an increased mixing of the Cu 4s²3d⁹ configuration when scalar relativity is included since this atomic state is then lowered relative to 4s¹3d¹⁰. On the other hand, the effects due to 3s3p correlation are nearly negligible, as is often assumed for the late transition metals. The final CCSD(T)/CBS 3s3p correlated values are observed to be in excellent agreement with experiment, with the bond length being only slightly underestimated by about 0.003 Å and the harmonic frequency is too large by just ~4 cm⁻¹. The predicted value of D_e is well within the experimental error bars.

2. TiF and Cu₂

Results for TiF and Cu₂ are shown in Tables X and XI, respectively. Overall the results for TiF is very reminiscent of TiH (Table VII). The basis set dependence is modest, and the core-valence effect on r_e is large and negative. It should be noted that use of the valence basis sets for the 3s3p correlation in this case leads to an overestimate of ΔD_e by about 0.5 kcal/mol at the CBS limit. The final DK-CCSD(T)/CBS+3s3p results for r_e and ω_e are nearly identical with the experimental values, while the calculated D_e is at the lower end of the experimental range. The present *ab*

TABLE X. Summary of $X^4\Phi$ TiF CCSD(T) spectroscopic constants. The aug-cc-pVnZ(-DK) and aug-cc-pwCVnZ-DK basis sets were used for F.

Basis set	r_e (Å)	ω_e (cm ⁻¹)	D_e (kcal/mol)
Nonrelativistic, valence correlation			
cc-pVTZ	1.8755	635.4	128.01
cc-pVQZ	1.8746	638.3	129.67
cc-pV5Z	1.8737	639.3	130.14
CBS-val	1.8730	640.1	130.52
Scalar relativistic effects, [DK-CCSD(T)]-[NR-CCSD(T)]			
cc-pVTZ-(DK,NR)	-0.0021	-1.0	-1.29
cc-pVQZ-(DK,NR)	-0.0020	1.2	-1.29
cc-pV5Z-(DK,NR)	-0.0020	0.2	-1.30
CBS-rel	-0.0020	-0.6	-1.30
DK relativistic, F 1s+Ti 3s3p correlation effects (CV-valence)			
cc-pVTZ-DK	-0.0358	13.5	1.03
cc-pVQZ-DK	-0.0386	11.1	1.49
cc-pV5Z-DK	-0.0388	12.8	1.53
CBS-CV1	-0.0389	14.4	1.57
cc-pwCVTZ-DK	-0.0303	11.8	0.13
cc-pwCVQZ-DK	-0.0347	9.9	0.70
cc-pwCV5Z-DK	-0.0367	10.9	0.93
CBS-CV2	-0.0384	11.8	1.12
Total, CBS(val+rel+CV2)	1.8325	651.4	130.3
Expt. ^a	1.8311	650.7	137±8

^aReference 68. The *ab initio* ω_e value from this work was used to derive D_e . The experimental value shown for ω_e actually corresponds to $\nu_{01}=\omega_e-2\omega_e x_e$. The *ab initio* $\omega_e x_e$ from this work is 4.1 cm⁻¹, which yields an "experimental" ω_e of 658.9 cm⁻¹.

initio value, however, is expected to be the more reliable result in this case. Our results can be compared to the recent RCCSD(T) work of Koukounas *et al.*⁴⁶ who investigated several electronic states of TiF with a large ANO basis set on Ti using both coupled cluster and MRCI methods. In general, their results are in good overall agreement with the cc-pVQZ results of the present work, however, their core-valence correlation effects on D_e seem to be about a factor of 3 too large, 2.9 kcal/mol compared to 1.1 kcal/mol in the present work. As discussed above, this could mainly be due to different orbitals being used in their calculations.

For the copper dimer, both regular and diffuse augmented results at the nonrelativistic level are shown in Table XI since the latter was calculated to strongly impact the excitation energy and ionization potential of the Cu atom. For both the cc-pVnZ and aug-cc-pVnZ series, the NR-CCSD(T) bond length and dissociation energy converge from above and below, respectively, but the values calculated with the aug-cc-pVnZ basis sets exhibit faster convergence towards the CBS limit, presumably due to the importance of describing *sd* correlation effects, which require diffuse *f*-type functions³⁸ Thus, the resulting CBS limits are slightly different depending on the choice of basis set series. As in CuH, scalar relativity strongly decreases the bond length and increases the dissociation energy, while 3s3p correlation has a negligible effect. The final DK-CCSD(T)/CBS+3s3p spectroscopic constants agree well with the accurate experimental values, but the remaining errors, 0.003 Å in r_e , 3 cm⁻¹ in ω_e ,

TABLE XI. Summary of $X^1\Sigma_g^+$ Cu₂ CCSD(T) spectroscopic constants.

Basis set	r_e (Å)	ω_e (cm ⁻¹)	D_e (kcal/mol)
Nonrelativistic, valence correlation			
cc-pVTZ	2.2642	246.2	41.47
cc-pVQZ	2.2591	248.7	42.04
cc-pV5Z	2.2532	251.2	42.69
CBS-val1	2.2485	253.3	43.23
aug-cc-pVTZ	2.2584	250.5	42.51
aug-cc-pVQZ	2.2531	251.5	43.14
aug-cc-pV5Z	2.2516	252.7	43.52
CBS-val2	2.2505	253.7	43.83
Scalar relativistic effects, [DK-CCSD(T)]-[NR-CCSD(T)]			
cc-pVTZ-(DK,NR)	-0.0356	15.7	2.82
cc-pVQZ-(DK,NR)	-0.0349	15.2	2.77
cc-pV5Z-(DK,NR)	-0.0345	15.3	2.79
CBS-rel	-0.0342	15.4	2.81
DK relativistic, Cu 3s3p correlation effects (CV-valence)			
cc-pVTZ-DK	-0.0032	1.3	0.25
cc-pVQZ-DK	-0.0008	1.7	0.17
cc-pV5Z-DK	-0.0005	0.3	-0.04
CBS-CV1	-0.0004	-0.7	-0.22
cc-pwCVTZ-DK	0.0015	0.5	-0.17
cc-pwCVQZ-DK	0.0009	0.2	-0.21
cc-pwCV5Z-DK	0.0005	0.4	-0.23
CBS-CV2	0.0002	0.5	-0.25
Total, CBS(val2+rel+CV2)	2.216	269.6	46.4
Expt. ^a	2.2193	266.46	47.93±0.57

^aReference 69.

and ~1 kcal/mol in D_e , are presumably due to missing higher-order correlation effects that are not recovered by the CCSD(T) method.

One of the concerns of the present work involves the computationally expensive evaluation of the 3s3p correlation effects, which can strongly affect spectroscopic properties in the early transition metals. The results discussed above appear to suggest that the present valence-only sets do an adequate job in describing 3s3p correlation, but generally overestimate the effect on the spectroscopic constants. Given the excellent results by Bauschlicher¹⁴ on TiH with his valence optimized basis sets, which had very flexible *spd* contractions, perhaps the addition of only the tight *spd* functions from the cc-pwCVnZ basis sets to the cc-pVnZ sets might yield reliable core-valence results with much less computational cost than with the full cc-pwCVnZ basis sets. This has been carried out in the cases of TiH and TiF, and indeed cc-pVnZ+2s2p2d calculations (the 2s2p2d from the appropriate cc-pwCVnZ sets) yielded CV correlation effects intermediate between those obtained with cc-pVnZ and cc-pwCVnZ. It was also determined that elimination of the highest tight angular momentum function from the cc-pwCVnZ basis sets, e.g., the tight *g* function in the cc-pwCVTZ basis set, had a negligible effect on the resulting CV correlation contributions. Hence, while the cc-pwCVnZ basis sets are capable of achieving benchmark quality core-valence correlation effects, more economical alternatives may be possible. Finally, the possible effect of basis set su-

perposition error (BSSE) on the calculated CV contributions was also investigated by using the function counterpoise method.⁴⁷ Except for a slight improvement at the cc-pwCVTZ level for CuH and Cu₂, the effect of BSSE on the CV correlation effects was found to be nearly negligible.

IV. CONCLUSIONS

New correlation consistent basis sets have been developed for the first-row transition metal elements that display systematic convergence towards the complete basis set limit for a wide array of atomic and molecular properties. Both nonrelativistic basis sets (cc-pVnZ, $n=T, Q, 5$) and sets optimized with the Douglas-Kroll-Hess scalar relativistic Hamiltonian (cc-pVnZ-DK, $n=T, Q, 5$) have been developed. Additional functions have been determined to form diffuse function augmented versions of these two series (aug-cc-pVnZ and aug-cc-pVnZ-DK), as well as sets designed to accurately recover important $3s3p$ correlation effects (cc-pwCVnZ and cc-pwCVnZ-DK). Benchmark calculations of atomic excitation energies, ionization potentials, and electron affinities were carried out at the CCSD(T) level of theory. The new basis sets allowed the estimation of accurate CBS limits in each case, which facilitated the critical assessment of the effects of scalar relativity and $3s3p$ correlation, as well as the overall intrinsic accuracy of the CCSD(T) method for these properties. In particular, it was found that the CCSD(T) method was capable of chemical accuracy (within 1 kcal/mol) for both atomic excitation energies ($4s^2 \rightarrow 4s^1$) and ionization potentials, but the electron affinities proved to be more difficult, with errors ranging between 1.5 and 2.5 kcal/mol for Ti, V, and Fe. For each of the atomic properties studied, the basis set convergence rate was generally slower for the late transition metals (Mn-Zn) in comparison to those with a less than half-filled $3d$ shell (Sc-Cr). Some representative molecular calculations were also carried out, and these results essentially followed the same trends as those observed in the atomic excitation energies and ionization potentials. Hence, just as the correlation consistent basis sets for the main group elements have provided a clear route to accurate *ab initio* spectroscopy and thermochemistry, the new basis sets from this work are expected to facilitate accurate, reliable calculations involving the first-row transition metals. All of the basis sets presented in this work can be obtained from EPAPS,⁴⁸ but will also be made available for download from the Pacific Northwest National Laboratory (PNNL) basis set website, <http://www.emsl.pnl.gov/forms/basisform.html>, as well as by request from one of the authors (Peterson).

ACKNOWLEDGMENTS

This work was partially supported by the National Science Foundation under CHE-0111282. Partial support by the Division of Chemical Sciences in the Office of Basis Energy Sciences of the U.S. Department of Energy (DOE) is also gratefully acknowledged. Some of this research was performed in the William R. Wiley Environmental Molecular Sciences Laboratory (EMSL) at the Pacific Northwest National Laboratory (PNNL). Operation of the EMSL is funded

by the Office of Biological and Environmental Research in the U.S. DOE. PNNL is operated by Battelle Memorial Institute for the U.S. DOE. The authors would also like to thank Dr. David Feller for his critical reading of the manuscript and helpful discussions.

- ¹K. Jankowski, R. Becherer, P. S. Scharf, H. Schiffer, and R. Ahlrichs, *J. Chem. Phys.* **82**, 1413 (1985).
- ²J. Almlöf and P. R. Taylor, *J. Chem. Phys.* **86**, 4070 (1987).
- ³T. H. Dunning, Jr., *J. Chem. Phys.* **90**, 1007 (1989).
- ⁴D. E. Woon and T. H. Dunning, Jr., *J. Chem. Phys.* **98**, 1358 (1993); T. H. Dunning, Jr., K. A. Peterson, and A. K. Wilson, *ibid.* **114**, 9244 (2001).
- ⁵A. K. Wilson, K. A. Peterson, D. E. Woon, and T. H. Dunning, Jr., *J. Chem. Phys.* **110**, 7667 (1999).
- ⁶K. A. Peterson, *J. Chem. Phys.* **119**, 11099 (2003); K. A. Peterson, D. Figgien, E. Goll, H. Stoll, and M. Dolg, *ibid.* **119**, 11113 (2003).
- ⁷R. A. Kendall, T. H. Dunning, Jr., and R. J. Harrison, *J. Chem. Phys.* **96**, 6796 (1992); D. E. Woon and T. H. Dunning, Jr., *ibid.* **100**, 2975 (1994); D. E. Woon and T. H. Dunning, Jr., *ibid.* **103**, 4572 (1995).
- ⁸K. A. Peterson and T. H. Dunning, Jr., *J. Chem. Phys.* **117**, 10548 (2002).
- ⁹A. J. H. Wachters, *J. Chem. Phys.* **52**, 1033 (1970).
- ¹⁰P. J. Hay and W. R. Wadt, *J. Chem. Phys.* **82**, 299 (1985); P. J. Hay and W. R. Wadt, *ibid.* **82**, 270 (1985); W. J. Stevens, M. Krauss, H. Basch, and P. G. Jasien, *Can. J. Chem.* **70**, 612 (1992); K. D. Dobbs and W. J. Hehre, *J. Comput. Chem.* **8**, 861 (1987); A. V. Mitin, J. Baker, and P. Pulay, *J. Chem. Phys.* **118**, 7775 (2003); V. A. Rassolov, J. A. Pople, M. A. Ratner, and T. L. Windus, *ibid.* **109**, 1223 (1998); M. Dolg, U. Wedig, H. Stoll, and H. Preuss, *ibid.* **86**, 866 (1987); C. C. Lovallo and M. Klobukowski, *J. Comput. Chem.* **24**, 1009 (2003); V. Kellö and A. J. Sadlej, *Theor. Chim. Acta* **91**, 353 (1995); V. Kellö and A. J. Sadlej, *ibid.* **94**, 93 (1996); P. Neogrady, V. Kellö, M. Urban, and A. J. Sadlej, *ibid.* **93**, 101 (1996); F. Rakowitz, C. M. Marian, and L. Seijo, *J. Chem. Phys.* **111**, 10436 (1999); A. Schäfer, C. Huber, and R. Ahlrichs, *ibid.* **100**, 5829 (1994); F. Weigend, F. Furche, and R. Ahlrichs, *ibid.* **119**, 12753 (2003); M. M. Hurley, L. F. Pacios, P. A. Christiansen, R. B. Ross, and W. C. Ermler, *ibid.* **84**, 6840 (1986); T. Koga, H. Tatewaki, H. Matsuyama, and Y. Satoh, *Theor. Chem. Acc.* **102**, 105 (1999); T. Koga, H. Tatewaki, and O. Matsuoka, *J. Chem. Phys.* **115**, 3561 (2001).
- ¹¹T. Noro, M. Sekiya, T. Koga, and H. Matsuyama, *Theor. Chem. Acc.* **104**, 146 (2000).
- ¹²A. Ricca and C. W. Bauschlicher, Jr., *Theor. Chem. Acc.* **106**, 314 (2001).
- ¹³C. W. Bauschlicher, Jr., *Theor. Chim. Acta* **92**, 183 (1995).
- ¹⁴C. W. Bauschlicher, Jr., *Theor. Chem. Acc.* **103**, 141 (1999).
- ¹⁵M. Pykavy and C. van Wuelen, *J. Phys. Chem. A* **107**, 5566 (2003).
- ¹⁶M. Douglas and N. M. Kroll, *Ann. Phys. (N.Y.)* **82**, 89 (1974); G. Jansen and B. A. Hess, *Phys. Rev. A* **39**, 6016 (1989).
- ¹⁷W. H. Press, S. A. Teukolsky, W. T. Vetterling, and B. P. Flannery, *Numerical Recipes in FORTRAN: The Art of Scientific Computing*, 2nd ed. (Cambridge University Press, Cambridge, 1992).
- ¹⁸H.-J. Werner, P. J. Knowles, R. D. Amos *et al.*, MOLPRO, version 2002.6, a package of *ab initio* programs (Cardiff, 2002).
- ¹⁹P. J. Hay, *J. Chem. Phys.* **66**, 4377 (1977).
- ²⁰C. W. Bauschlicher, Jr. and P. R. Taylor, *Theor. Chim. Acta* **86**, 13 (1993).
- ²¹R. Pou-Amérgo, M. Merchán, I. Nebot-Gil, P.-O. Widmark, and B. O. Roos, *Theor. Chim. Acta* **92**, 149 (1995).
- ²²H. Partridge, *J. Chem. Phys.* **90**, 1043 (1989).
- ²³K. Ruedenberg, R. C. Raffanetti, and R. D. Bardo, in *Energy, Structure and Reactivity, Proceedings of the 1972 Boulder Conference on Theoretical Chemistry* (Wiley, New York, 1973); D. F. Feller and K. Ruedenberg, *Theor. Chim. Acta* **52**, 231 (1979).
- ²⁴H. Partridge and K. Faegri, Jr., *Theor. Chim. Acta* **82**, 207 (1992).
- ²⁵H. Tatewaki, T. Koga, and S. Yamamoto, *Theor. Chem. Acc.* **105**, 55 (2000).
- ²⁶H. Partridge, NASA Technical Memorandum Report No. 101044, 1989.
- ²⁷G. A. Petersson, S. Zhong, J. A. Montgomery, Jr., and M. J. Frisch, *J. Chem. Phys.* **118**, 1101 (2003).
- ²⁸M. J. Frisch, G. W. Trucks, H. B. Schlegel *et al.*, Gaussian 03, revision C.02, Gaussian, Inc., Wallingford, CT, 2004.
- ²⁹D. L. Strout and T. H. Dunning, Jr. (unpublished).
- ³⁰C. W. Bauschlicher, Jr., *Chem. Phys. Lett.* **305**, 446 (1999).

- ³¹ H. Tatewaki and T. Koga, *Chem. Phys. Lett.* **228**, 562 (1994).
- ³² J. M. Garcia de la Vega, *J. Phys. B* **27**, L447 (1994); T. Koga, H. Tatewaki, and A. J. Thakkar, *J. Chem. Phys.* **100**, 8140 (1994).
- ³³ K. Raghavachari, G. W. Trucks, J. A. Pople, and M. Head-Gordon, *Chem. Phys. Lett.* **157**, 479 (1989).
- ³⁴ M. Rittby and R. J. Bartlett, *J. Phys. Chem.* **92**, 3033 (1988); G. E. Scuseria, *Chem. Phys. Lett.* **176**, 27 (1991); P. J. Knowles, C. Hampel, and H.-J. Werner, *J. Chem. Phys.* **99**, 5219 (1994); M. J. O. Deegan and P. J. Knowles, *Chem. Phys. Lett.* **227**, 321 (1994).
- ³⁵ K. A. Peterson, D. E. Woon, and T. H. Dunning, Jr., *J. Chem. Phys.* **100**, 7410 (1994).
- ³⁶ T. Helgaker, W. Klopper, H. Koch, and J. Noga, *J. Chem. Phys.* **106**, 9639 (1997); A. Halkier, T. Helgaker, P. Jørgensen, W. Klopper, H. Koch, J. Olsen, and A. K. Wilson, *Chem. Phys. Lett.* **286**, 243 (1998); W. Klopper, K. L. Bak, P. Jørgensen, J. Olsen, and T. Helgaker, *J. Phys. B* **32**, R103 (1999).
- ³⁷ K. Raghavachari, K. K. Sunil, and K. D. Jordan, *J. Chem. Phys.* **83**, 4633 (1985).
- ³⁸ C. W. Bauschlicher, Jr., S. P. Walch, and S. R. Langhoff, in *Quantum Chemistry: The Challenge of Transition Metals and Coordination Chemistry*, edited by A. Veillard (Reidel, Dordrecht, 1986), p. 15.
- ³⁹ T. Koga, H. Aoki, J. M. Garcia de la Vega, and H. Tatewaki, *Theor. Chem. Acc.* **96**, 248 (1997).
- ⁴⁰ N. B. Balabanov and K. A. Peterson (unpublished).
- ⁴¹ C. W. Bauschlicher, Jr. and G. L. Gutsev, *Theor. Chem. Acc.* **108**, 27 (2002).
- ⁴² N. Miura, T. Noro, F. Sasaki, and Y. Osanai, *Theor. Chem. Acc.* **99**, 248 (1998).
- ⁴³ Y. Osanai, H. Ishikawa, N. Miura, and T. Noro, *Theor. Chem. Acc.* **105**, 437 (2001).
- ⁴⁴ J. L. Dunham, *Phys. Rev.* **41**, 721 (1932).
- ⁴⁵ S. P. Walch and C. W. Bauschlicher, Jr., *J. Chem. Phys.* **78**, 4597 (1983); S. R. Langhoff, C. W. Bauschlicher, Jr., and A. P. Rendell, *J. Mol. Spectrosc.* **138**, 108 (1989); C. M. Marian, *J. Chem. Phys.* **94**, 5574 (1991); R. Pou-Amérigo, M. Merchán, I. Nebot-Gil, P.-Å. Malmqvist, and B. O. Roos, *ibid.* **101**, 4893 (1994); C. L. Collins, K. G. Dyall, and H. F. Schaefer, III, *ibid.* **102**, 2024 (1995); V. Barone and C. Adamo, *Int. J. Quantum Chem.* **61**, 443 (1997); J. Hrusak, S. Ten-no, and S. Iwata, *J. Chem. Phys.* **106**, 7185 (1997); A. I. Boldyrev and J. Simons, *J. Mol. Spectrosc.* **188**, 138 (1998); C. van Wuellen, *J. Chem. Phys.* **109**, 392 (1998); C. J. Barden, J. C. Rienstra-Kiracofe, and H. F. Schaefer, III, *ibid.* **113**, 690 (2000); S. Yanagisawa, T. Tsuneda, and K. Hirao, *ibid.* **112**, 545 (2000); S. Koseki, Y. Ishihara, H. Umeda, D. G. Fedorov, and M. S. Gordon, *J. Phys. Chem. A* **106**, 785 (2002); G. L. Gutsev and C. W. Bauschlicher, Jr., *ibid.* **107**, 4755 (2003); X. Wang and L. Andrews, *ibid.* **107**, 4081 (2003); D. J. D. Wilson, C. J. Marsden, and E. I. von Nagy-Felsobuki, *Phys. Chem. Chem. Phys.* **5**, 252 (2003).
- ⁴⁶ C. Koukounas, S. Kardahakis, and A. Mavridis, *J. Chem. Phys.* **120**, 11500 (2004).
- ⁴⁷ S. F. Boys and F. Bernardi, *Mol. Phys.* **19**, 553 (1970).
- ⁴⁸ See EPAPS Document No. E-JCPSA6-123-315526 for Gaussian exponents and contraction coefficients for the following basis sets: cc-pVnZ-DK, cc-pVnZ, cc-pwCVnZ-DK, cc-pwCVnZ, and their associated diffuse functions. $n=T, Q$, and 5 in each case. This document can be reached via a direct link in the online article's HTML reference section or via the EPAPS homepage (<http://www.aip.org/pubservs/epaps.html>).
- ⁴⁹ C. E. Moore, *Atomic Energy Levels* (NSRDS-NBS 35, Office of Standard Reference Data, National Bureau of Standards, Washington, DC, 1971).
- ⁵⁰ T. Andersen, H. K. Haugen, and H. Hotop, *J. Phys. Chem. Ref. Data* **28**, 1511 (1999).
- ⁵¹ J. Sugar and C. Corliss, *J. Phys. Chem. Ref. Data* **14**, 1 (1985).
- ⁵² J. E. Sohl, Y. Zhu, and R. D. Knight, *J. Opt. Soc. Am. B* **7**, 9 (1990).
- ⁵³ A. M. James, P. Kowalczyk, E. Langlois, M. D. Campbell, A. Ogawa, and B. Simard, *J. Chem. Phys.* **101**, 4485 (1994).
- ⁵⁴ R. H. Page and C. S. Gudeman, *J. Opt. Soc. Am. B* **7**, 1761 (1990).
- ⁵⁵ H.-P. Looock, L. M. Beaty, and B. Simard, *Phys. Rev. A* **59**, 873 (1999).
- ⁵⁶ C. M. Brown, S. G. Tilford, and M. L. Ginter, *J. Opt. Soc. Am. B* **65**, 385 (1975).
- ⁵⁷ C. S. Feigerle, R. R. Corderman, S. V. Bobashev, and W. C. Lineberger, *J. Chem. Phys.* **74**, 1580 (1981).
- ⁵⁸ R. N. Ilin, V. I. Sakharov, and I. T. Serenkov, *Opt. Spektrosk.* **62**, 976 (1987).
- ⁵⁹ R. C. Bilodeau, M. Scheer, and H. K. Haugen, *J. Phys. B* **31**, 3885 (1998).
- ⁶⁰ D. G. Leopold and W. C. Lineberger, *J. Chem. Phys.* **85**, 51 (1986).
- ⁶¹ M. Scheer, C. A. Brodie, R. C. Bilodeau, and H. K. Haugen, *Phys. Rev. A* **58**, 2051 (1998).
- ⁶² N. Andersson, W. J. Balfour, P. F. Bernath, B. Lindgren, and R. S. Ram, *J. Chem. Phys.* **118**, 3543 (2003).
- ⁶³ Y.-M. Chen, D. E. Clemmer, and P. B. Armentrout, *J. Chem. Phys.* **95**, 1228 (1991).
- ⁶⁴ R.-D. Urban and H. Jones, *Chem. Phys. Lett.* **178**, 295 (1991).
- ⁶⁵ L. S. Sunderlin and P. B. Armentrout, *J. Phys. Chem.* **94**, 3589 (1990).
- ⁶⁶ R. S. Ram, P. F. Bernath, and J. W. Brault, *J. Mol. Spectrosc.* **113**, 269 (1985).
- ⁶⁷ R. Georgiadis, E. R. Fisher, and P. B. Armentrout, *J. Am. Chem. Soc.* **111**, 4251 (1989).
- ⁶⁸ R. S. Ram, J. R. D. Peers, Y. Teng, A. G. Adam, A. Muntianu, P. F. Bernath, and S. P. Davis, *J. Mol. Spectrosc.* **184**, 186 (1997); K. F. Zmbov and J. L. Margrave, *J. Phys. Chem.* **71**, 2893 (1967).
- ⁶⁹ R. S. Ram, C. N. Jarman, and P. F. Bernath, *J. Mol. Spectrosc.* **156**, 468 (1992); E. A. Rohlfing and J. J. Valentini, *J. Chem. Phys.* **84**, 6560 (1986).